2018

Development of a nonlinear adaptive absorber based on magnetorheological elastomer

Shuaishuai Sun
University of Wollongong, ss886@uowmail.edu.au

Jian Yang
University of Wollongong, jy937@uowmail.edu.au

Tanju Yildirim
Shenzhen University, ty370@uowmail.edu.au

Haiping Du
University of Wollongong, hdu@uow.edu.au

Gursel Alici
University of Wollongong, gursel@uow.edu.au

See next page for additional authors

Development of a nonlinear adaptive absorber based on magnetorheological elastomer

Abstract

The resonance shift property of magnetorheological elastomer is important for developing adaptive absorbers. However, it is well-known that passive nonlinear absorbers have wider effective frequency bandwidths. This article combines these two characteristics in order to develop a hybrid magnetorheological elastomer absorber which can shift its natural frequency and has a wider absorption bandwidth under each constant current. The adaptability and nonlinearity were fully verified experimentally. Afterwards, the absorption ability of the hybrid magnetorheological elastomer absorber was investigated and analyzed. The results show that the effective bandwidth of this absorber is broadened under certain levels of current than linear absorber, and this is caused by the presence of nonlinearity; and the adaptability induced by the magnetorheological elastomer undoubtedly empowers the absorber possible to trace the excitation frequency changing in real time. A short-time Fourier transform was finally used to control the magnetorheological elastomer absorber to verify its controllability, showing that an optimal absorption transmissibility was achieved by the controlled hybrid absorber.

Publication Details

Sun, S., Yang, J., Yildirim, T., Du, H., Alici, G., Zhang, S. & Li, W. (2018). Development of a nonlinear adaptive absorber based on magnetorheological elastomer. Journal of Intelligent Material Systems and Structures, 29 (2), 194-204.

Authors

Shuaishuai Sun, Jian Yang, Tanju Yildirim, Haiping Du, Gursel Alici, Shiwu Zhang, and Weihua Li

Development of a new nonlinear adaptive absorber based on magnetorheological elastomer

S.S. Sun[1], J. Yang[1], T. Yildirim[1], H. Du[2], G. Alici[1], S.W. Zhang[3], and W.H. Li[1]

Abstract

The resonance shift property of magnetorheological elastomer (MRE) is important for developing adaptive absorbers. On the other hand, it is well known that passive nonlinear absorbers have wider effective frequency bandwidths. This paper combines these two characteristics in order to develop a hybrid MRE absorber which can shift its natural frequency and has a wider absorption bandwidth under each constant current. The adaptability and nonlinearity were fully verified experimentally. Afterwards, the absorption ability of the hybrid MRE absorber was investigated and analysed. The results show that the effective bandwidth of this absorber is broadened under certain levels of current than linear absorber and this is caused by the presence of nonlinearity; and that the adaptability induced by the MRE undoubtedly empowers the absorber possible to trace the excitation frequency changing in real time. A short time Flourier transform (STFT) was finally used to control the MRE absorber to verify its controllability, showing that an optimal absorption transmissibility was achieved by the controlled hybrid absorber.

Keywords

Vibration control, adaptive absorber, MRE, nonlinearity

Introduction

Absorbers have been commonly acknowledged in the engineering industry as a way of absorbing vibrational energy from machinery or structure (Lee, et al., 2001, Liu and Liu, 2005, Yang et al., 2014b Weber, 2014). The concept of a vibration absorber was first proposed by Frahm (H, 1911). Consisting of a mass and a stiffness element with appropriate damping, the vibration absorber is undoubtedly a simple, economic, and reliable way to suppress vibration. The working principle of an absorber is to transfer the vibrational energy of the controlled objects to the oscillators by equaling its natural frequency to the frequency of the disturbing vibration. This means that the effectiveness of an absorber lies in the natural frequency bandwidth that it achieves. By slightly widening the operation bandwidth, the performance will improve dramatically. In order to improve the functionality of a vibration absorber, it is important to broaden the operation bandwidth because the vibration sources in the practical circumstances are usually frequency variant or cover a large frequency range.

[1]School of Mechanical, Materials and Mechatronic Engineering, University of Wollongong, NSW, Australia

[2]School of Electrical, Computer and Telecommunications Engineering, University of Wollongong, NSW, Australia

[3]Department of Precision Machinery and Precision Instrumentation, University of Science and Technology of China, Hefei, Anhui province, China

Corresponding authors:

Weihua Li, School of Mechanical, Materials and Mechatronic Engineering, University of Wollongong, Wollongong, NSW, Australia. Email: weihuali@uow.edu.au

Shiwu Zhang, Department of Precision Machinery and Precision Instrumentation, University of Science and Technology of China, Hefei, Anhui province, China. Email: swzhang@ustc.edu.cn

In order to increase the effective bandwidth of the absorber, active absorbers and semi-active absorbers have been used (Davis and Lesieutre, 2000, Walsh and Lamancusa, 1992) but the active devices are less used because of their high requirements in terms of power, cost and maintenance. On the other hand, semi-active absorbers are more widely used because of their simplicity, robustness, and reliability. Magnetorheological elastomers (MREs), as a smart material whose stiffness is controllable (Xing et al., 2015, Yang et al., 2013, Yang et al., 2014a, Li and Li, 2015), are currently widely used because the involvement of MREs allows the absorber to be tuned in real time by changing the stiffness (Li et al., 2014, Popp et al., 2010, Ginder et al., 2001, Sun et al., 2015a). This semi-active property enables the absorber to adapt to vibration sources which vary according to their frequency. Deng developed an MRE absorber working in shear mode, whose natural frequency can vary from 55 to 82 Hz (Deng et al., 2006, Deng and Gong, 2008). Subsequently, Gong's group applied a voice motor on an MRE absorber in order to counteract the effect of damping and increase the absorber's effectiveness (Peng and Gong, 2013, Liao et al., 2011). As a way to further improve and complete the MRE based absorber, Sun et al. developed a multilayered MRE absorber which is much better at dealing with vibrations with larger amplitude (Sun et al., 2015b, Sun et al., 2015c). The effective frequency bandwidth of the MRE absorber under certain constant current, however, is still narrow although it can tune its natural frequency to track the excitation frequency. In other words, the MRE absorber can attenuate the vibration with single frequency well but cannot effectively suppress the vibration with multiple frequencies because the MRE absorber can only match one frequency at a time and this means that it is necessary to find a way to overcome this problem. To solve the problem of the limitations of the MRE absorber, using nonlinear stiffness is a promising method. The passive nonlinear absorber has been shown to be more effective and has wider effective frequency bandwidth than its linear counterpart. Roberson (1952) did the pioneer research into an undamped nonlinear dynamic vibration absorber which consists of a linear absorber and a hardening cubic spring. The investigation results prove that the vibration suppression bandwidth of the nonlinear absorber is much wider than a linear one. This conclusion was experimentally verified by Arnold (1955). Following Roberson's research, Snowdon (1959) further improved the performance of the nonlinear absorber by adding a fixed damping factor and a spring the stiffness of which was proportional to the excitation frequency. The results have confirmed the improved nonlinear absorber can better reduce the resonance of the primary structure. Tang applied magnets to the energy harvesting system, which can be used as an absorber as well (Tang and Yang, 2012). The experimental results verified that the magnetic system's induced nonlinearity can broaden the effective frequency range. Further research into nonlinear absorbers has been done in recent years (Starosvetsky and Gendelman, 2008, Yildirim et al., 2016) and this research has fully confirmed that the effective frequency bandwidth of passive nonlinear absorbers is wider than passive ones. As a result, introducing nonlinearity to the MRE absorber can create an adaptive nonlinear vibration absorber which will not only have wider working bandwidth under each fixed current but also is able to shift the resonance in order to adapt to the excitation variation.

In order to introduce nonlinearity to the MRE absorber, two opposite polar magnets were introduced to the linear MRE absorber. The combination of the MRE structure and the permanent magnets contributes to both the adaptability and the nonlinearity. This article firstly detailed the configuration of the absorber and its design process. Then its nonlinearity and adaptability were evaluated. A three story building model was used to evaluate the absorption effectiveness of the absorber. The last part provides a summary of this paper.

Structure, working principle and design process of the MRE absorber

Structure

Based on the design of the linear multilayered MRE absorber, the nonlinear MRE absorber is developed by introducing magnetic interaction. As shown in Figure 1, it is mainly composed of two parts: the MRE structure on the left of the figure and the nonlinearity generation part on the right. The weight ratio of the iron particles, silicon rubber and silicon oil used for the MRE fabrication is 7:2:1. The MRE structure has a solenoid and a multilayered MRE inside the steel yoke, vertically. Surrounding the steel yoke, a plastic supporter is fixed to the yoke as a connection to the rotary arm. The nonlinearity is generated by the relative motion of the two permanent magnets. One of the magnets is connected to the MRE structure through the rotary arm. The other is embedded into the plastic structure which is fixed to the bottom plate of the absorber. The two magnets generate attractive force between them. A round ring is mounted between the bottom plate and the solenoid in order to guarantee that the MRE absorber works in an angular direction. The detailed size of the nonlinear MRE absorber is shown in Table 1. The m_1 and m_2 are the magnetic moments of the two magnets. The prototype of the hybrid MRE absorber is shown in Figure 2.

Table.1. Parameters of the nonlinear MRE absorber

Parameters	Values		Parameters	Values
h_1	45 mm		L_1	5 mm
h_2	1 mm		L_2	100 mm
d_1	90mm		L_3	5 mm
d_2	35mm		L_4	5 mm
l_1	120mm		Coil turns	1000
m_1	0.258		l_2	100mm
m_2	0.258		J	0.0151 kg*m^2

Working principle

Generally speaking, the working principle of an absorber is that the vibration energy of the primary system can be transferred to the absorber when the absorber's natural frequency equals to the excitation frequency and subsequently the vibration of the primary system can be suppressed. The proposed hybrid MRE absorber works in an angular direction and its angular motion will be used to absorb the vibration energy from the control object. This absorber mainly contains two parts, including the MRE structure and the nonlinearity component. The MRE structure is used to achieve adaptability because of the variability of the MRE's stiffness in response to variations in the magnetic field. The natural frequency of the hybrid absorber can be controlled by the solenoid current. The multilayered MRE structure enables the absorber to have greater angular flexibility and this ensures the high vibration absorption capability (Sun et al., 2015b, Yang et al., 2014a). The presence of the steel sheets also enhances the magnetic induction of the MRE and strengthens the vertical support.

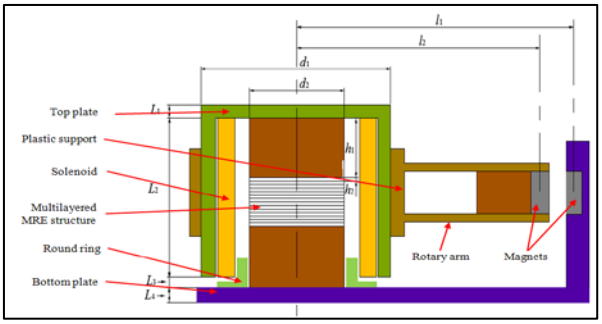

Figure 1 Structure of the hybrid MRE absorber

Figure 2 The prototype of the hybrid MRE absorber

The nonlinearity component, forming by a pair of magnets, is responsible for introducing nonlinearity to the system because the interaction force between the magnets is nonlinear. The magnet-induced nonlinearity will significantly change the behavior

and the performance of the absorber. As shown in Figure 3, the permanent m_1 was fixed to the bottom plate and remains relatively motionless with the bottom plate under external excitation while the magnet, m_2, will move angularly around the center point of the MRE structure, O, due to the angular flexibility of the MRE structure. The distance between the two magnets keeps changing, thereby generating a nonlinear magnetic force which, in turn, influences the movement of the MRE structure.

In summary, the working principle of the hybrid MRE absorber is that the MRE structure provides adaptability for the hybrid MRE absorber allowing it to track the changing dominant excitation frequency while the nonlinearity widens the effective frequency bandwidth of the hybrid MRE absorber under each constant current.

Design process of the MRE absorber

Two factors have to be taken into account when designing the absorber. One is its adaptability in response to the varying current levels. The other is its effective bandwidth under constant current levels. A balanced relationship must be built between the two factors when designing the absorber.

As the first step to design the hybrid absorber, its resonance frequency variation corresponding to different currents were designed and calculated. The detailed design procedure is presented as follows.

Based on Sun et al., 2015b, the increased shear modulus of MRE under different magnetic fields (current levels) can be obtained by:

$$\Delta G = 36\phi\mu_o\mu_l\beta^2\vec{H}_o^{\,2}\left(\frac{a}{d}\right)^3\zeta \quad (1)$$

where $\mu_p \approx 1000$ and $\mu_l \approx 1$ are the relative permeability of the iron particles and silicon rubber, respectively, μ_o is the vacuum permeability. $\beta = (\mu_p - \mu_l)/(\mu_p + 2\mu_l) \approx 1$, a= 4.3*10^{-6}m is the average particle radius, $\phi = 0.25$ is the volume fraction, d= 5.5*10^{-6}m is the particle distance before deflection, $\vec{H}_o$ is the intensity of the applied magnetic field, and $\zeta = \sum_{j=1}^{n}\frac{1}{j^3} \approx 1.202$.

The torsional stiffness of the ith MRE sheet can be written as:

$$K_{ri} = \frac{GI_p}{L} = \frac{(G_o+\Delta G)I_p}{L} = \frac{(G_o+36\phi\mu_o\mu_l\beta^2\vec{H}_o^{\,2}\left(\frac{a}{d}\right)^3\zeta)I_p}{L} \quad (2)$$

where G_o is the initial shear modulus of MRE, G is the overall shear modulus, L is the thickness of the MRE sheet. I_p is the polar moment of inertia of the MRE layer and can be calculated by:

$$I_p = \pi d_2^{\,4}/32 \quad (3)$$

where d_2 is the diameter of the MRE layer.

The torsional stiffness of the whole laminated MRE pillar (10 layers of MRE sheet) can be calculated by the following equation:

$$\frac{1}{k_{rw}} = \sum_{i=1}^{10}\frac{1}{k_{ri}} + \sum_{j=1}^{10}\frac{1}{k_{rj}} \quad (4)$$

where k_{rw} is the overall torsional stiffness of the laminated MRE pillar, k_{rj} is the torsional stiffness of steel sheet. It is known that $k_{ri} \ll k_{rj}$, therefore k_{rw} can be simplified as:

$$k_{rw} = \frac{k_{ri}}{10} \quad (5)$$

The magnetic field $\vec{H}_o$ in equation (1) can be calculated by the calculation method in (Sun et al., 2015b):

$$NI = B_{MRE}S_{MRE}R_m \quad (6)$$

$$B_{MRE} = \mu_{MRE}\vec{H}_o \quad (7)$$

$$R_m = R_1 + R_2 + R_3 + R_4 + R_5 \quad (8)$$

where NI is the magnetomotive force of coil, B_{MRE} is the magnetic flux density passing through MRE and S_{MRE} is the flux area of MRE. R_1, R_2, R_3, R_4, and R_5 are magnetic resistances of ten MRE layers, two steel pillars, air gap, steel yoke, top and bottom plates, respectively. In summary, the resonance frequency shift property of the hybrid absorber can be designed on the basis of the above analysis.

The design of the nonlinearity component will be the second step to design the hybrid absorber. The nonlinear force *F* between the two magnets can be calculated according to the classic dipole–dipole magnetic interaction (Levitt, 2001):

$$F = \frac{3\mu_0}{4\pi|r|^4}\left((\hat{r}\times m_1)\times m_2 + (\hat{r}\times m_2)\times m_1 - 2\hat{r}(m_2\cdot m_1) + 5\hat{r}((\hat{r}\times m_1)\cdot(\hat{r}\times m_2))\right) \quad (9)$$

where r̂ is a unit vector parallel to the line joining the centers of the two dipoles, and |r| is the distance between the centers of m_1 and m_2. m_1, m_2, and l_2 remain constant while α, θ , and r̂ change dynamically.

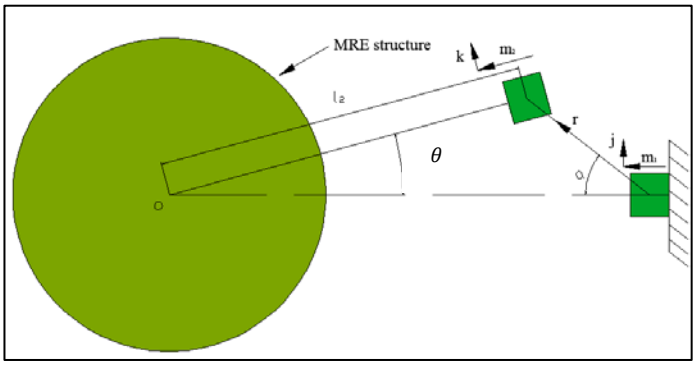

Figure 3. The magnetic interaction of the two magnets

According to the geometry relationship in Figure 3, the magnetic interaction force in unit vector k direction can be shown as:

$$F = \frac{3\mu_0}{4\pi|r|^4}(|m_1||m_2|\sin(\alpha) + |m_1||m_2|\sin(\alpha + \theta)\cos(\theta) + 2|m_1||m_2|\sin(\alpha + \theta)\cos(\theta) - 5|m_1||m_2|\sin(\alpha + \theta)\sin(\alpha)\sin(\alpha + \theta)) \quad (10)$$

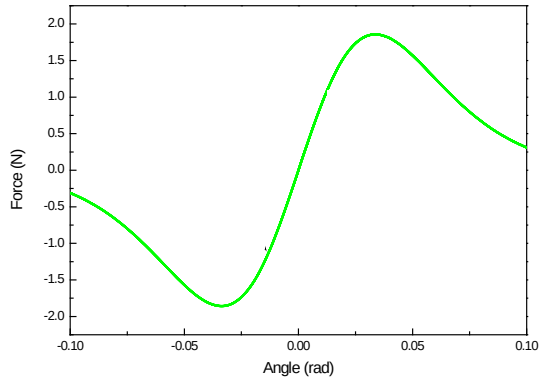

Figure 4 Relationship between the magnetic force and rotary angle

From Equation (10), the relationship between the magnetic force and the relative angle θ was simulated and is shown in Figure 4. The parameters used in this simulation are based on the real size of the hybrid MRE absorber, as shown in Table 1. It can be seen that the relationship is highly nonlinear.

Based on the calculations of the MRE stiffness and magnets induced nonlinear force, the dynamic equation of the nonlinear MRE absorber can be built, which is:

$$J\ddot{\theta}_2 + k_{rw}(\theta_2 - \theta_1) + c(\dot{\theta}_2 - \dot{\theta}_1) + Fl_2 = 0 \quad (11)$$

where J is the moment of inertia of the oscillator, c is the damping of the nonlinear MRE absorber, θ_2 is the torsional response of the oscillator of the MRE absorber, θ_1 is the torsional excitation.

The design criteria of the nonlinear MRE absorber include two rules: (a) maximising the effective frequency bandwidth under certain constant current using nonlinearity; and (b) achieving high adaptability using MRE material. However, these two criteria are conflicting to each other, which means the higher nonlinearity can expand the effective frequency bandwidth of the absorber under certain current but also decreases the natural frequency shift range under different current levels. In order to optimise the two criteria, the following analysis of the nonlinear MRE absorber on the basis of the dynamic Eq.11 has been conducted. This equation is solved by the Runge-Kutta method available in MATLAB/Simulink. In order to theoretically analyse the effects of the MRE stiffness and the nonlinearity on the performance of the hybrid MRE absorber, current level (magnetic field) and the rotary arm length l_2 are chosen to adjust the MRE stiffness and nonlinearity. The increases of the current level and the arm length lead to the increase of MRE stiffness and nonlinearity of the hybrid absorber, respectively. Figures 5 and 6 present the simulation results, which indicate the influence of rotary arm length l_2 on the effective bandwidth under a constant MRE stiffness 4 Nm/rad and 11 Nm/rad, respectively. These figures compare the performances of nonlinear absorbers with linear absorber. It can be seen from Figure 5 that the effective frequency bandwidth of the nonlinear absorber is wider than linear absorber and increasing nonlinearity by increasing the arm length leads to wider effective bandwidth. Specifically, the frequency bandwidth of the nonlinear absorber with 0.2m rotary arm reaches 2.7Hz while the linear one only reaches 0.9Hz, as

indicated in Figure 5. Figures 7 and 8 show the performance of the absorber under varying current levels and fixed arm lengths. It can be seen that the resonance point shifts to the right of x axis as the current increases, indicating that the resonance frequency of the absorber is controllable. We can also obtain the frequency shift range from the two figures. The relative change is 1.2Hz when l_2 equals to 0.1m and 1Hz when l_2 equals to 0.2m. Subsequently, it can be concluded that increasing rotary arm length decreases frequency shift range. This means that conflicting occasions happen between these two parameters and appropriate values should be chosen according to different application cases. In this application case with three story building, parameters listed in Table 1 are chosen according to the requirements of the building vibration control.

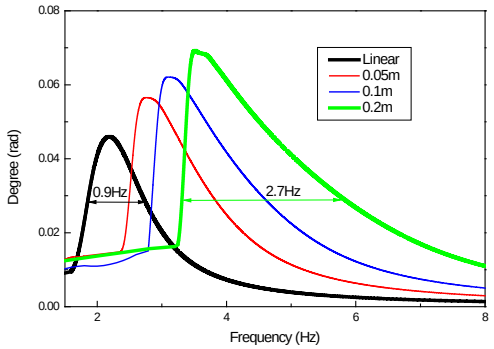

Figure 5 Influence of the nonlinearity when MRE stiffness is 4 Nm/rad

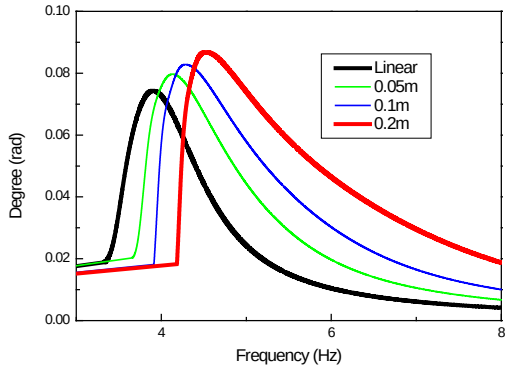

Figure 6 Influence of the nonlinearity when MRE stiffness is 11 Nm/rad

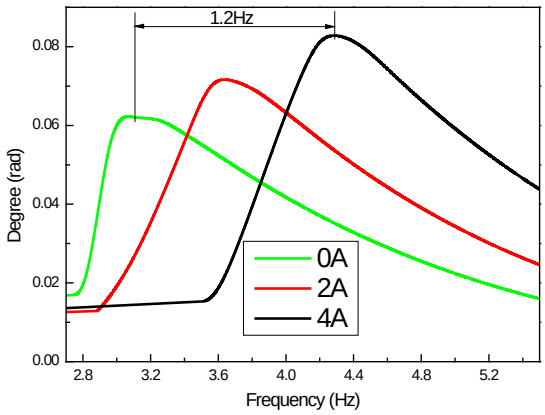

Figure 7 Influence of the varying current when the arm length is 0.1m

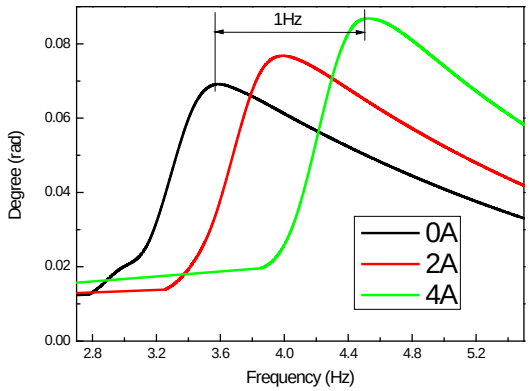

Figure 8 Influence of the varying current when the arm length is 0.2m

Experimental test of the hybrid MRE absorber

Experiment setup

Experimental tests were conducted to study the dynamic properties of the proposed nonlinear MRE absorber. Figure 9 shows the experimental set up. The absorber was fixed onto the vibration platform driven by a shaker (VTS, .VC 100-8). Two accelerometers (CA-YD-106) were used to measure the accelerations of the excitation and the oscillator, respectively. It should be noted that the accelerometer for the oscillator is mounted on the rotary arm in order to measure the acceleration in an angular direction. A DC power supply (THURLBY-

THANDAR, INSTRUMENTS LTD) was used to provide current to the absorber solenoid. A data acquisition (DAQ) board was used as the interface between the hardware and the software and this transferred the measured accelerations to the computer. The signal collection, recording, and processing systems were developed using the LabVIEW program.

When the shaking table is driven to vibrate horizontally, the MRE structure starts to rotate around its center, and as a result, the attached magnet will oscillate. This means that the distance between the two magnets will change and nonlinearity will appear.

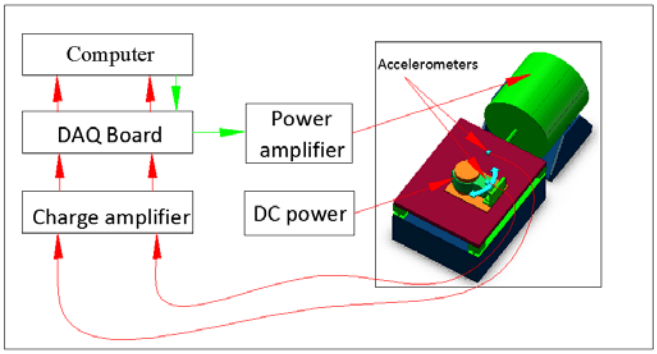

Figure 9. Experimental setup for characterizing the absorber

Testing Result

Frequency shift performance

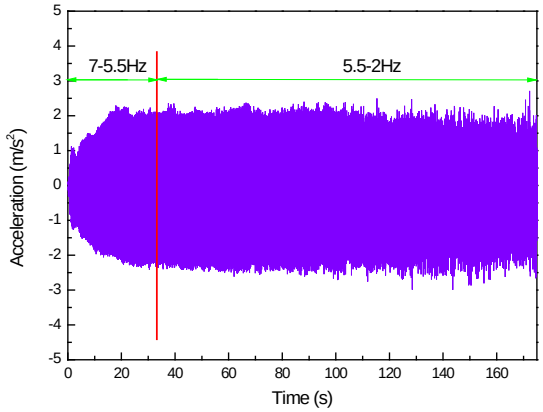

Figure 10 Excitation signal

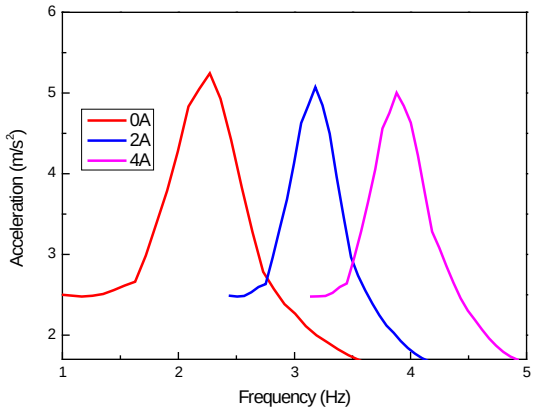

Figure 11 Responses of linear absorber under various current levels

Adaptability verification

The frequency shift performance of both linear and nonlinear absorbers was carried out, where a sinusoidal signal, as shown in Figure 10, with a frequency range from 5.5 Hz to 2 Hz with an amplitude of 2.5m/s^2 was used to excite the absorbers. A PID controller is used to control the excitation to guarantee its stability. It is noticed that excitation was started from 7Hz to make sure the amplitude of the excitation stabilises at 2.5m/s^2 from 5.5Hz to 2Hz. The acceleration response under various current levels from 0A to 4A was collected, as shown in Figure 11. It can be seen that the responses are all linear. The resonance frequency increases from 2.2 Hz to 4 Hz as the current grows from 0A to 4A, and this demonstrates its adaptability under linear working mode.

Figure 12 shows the frequency shift response of the nonlinear absorber under the same excitation and the applied current varies from 0A to 4A with a step of 2A. For each current level, the acceleration changes abruptly at the resonance frequency. The resonance frequency shifts from 3.5Hz to 4.6Hz. The relationships between the current and natural frequency of the linear and nonlinear MRE absorber both are shown in Figure 13. It can be seen from this figure that the model presented in section “Design process of the MRE absorber” can predict the frequency shift properties well, and this verified

the correctness of the theoretical calculation in that section.

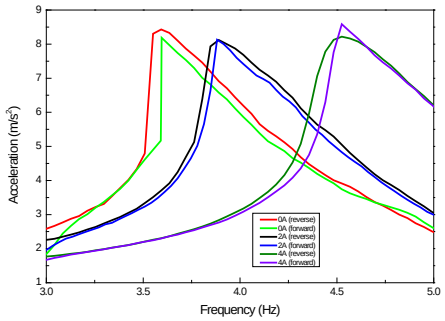

Figure 12 Responses of nonlinear absorber under various current levels

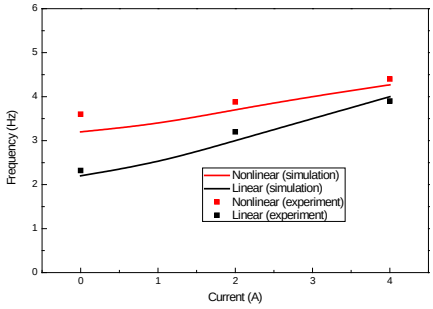

Figure 13. Comparison between experiment and calculation

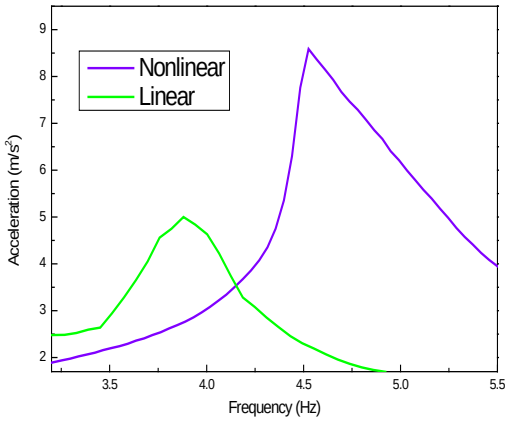

Figure 14 Response comparison between the linear and nonlinear absorber.

Figure 14 compares the transmissibility of the linear absorber with nonlinear absorber when the current level was 4A. It can be seen that under the same current level nonlinear transmissibility has wider bandwidth than the linear case, which verified the advantage of the nonlinear absorber experimentally.

Vibration reduction evaluation

The adaptability and the nonlinearity of the proposed MRE absorber have been verified. This section aims to evaluate its vibration reduction capability.

Figure 16 shows the photograph of the experimental setup. This testing system is similar to that introduced in Section 4 since the same hardware and software were used, with only one exception that a three story building model was included in this system as the control object. This three story building system consists of three steel plates working as three levels of the building. The mass of the scaled building is 12kg. The mass of the absorber is 3kg, and the mass ratio between the absorber and primary system is 0.25. This three story building was designed and built with a length scale factor of 1:12. The height of the scaled building was 0.5 m, which corresponds to a real three story building approximately 6m high. All the variables and dimensions were scaled down according to the scaling laws (Mills, 1979). The scaled building was fixed to the shaking table. Then the nonlinear MRE absorber was mounted on the top steel plate. Two accelerometers measured the accelerations of the top floor and the excitation, respectively.

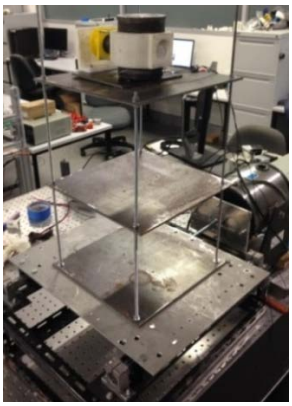

Figure 15. Vibration attenuation evaluation system

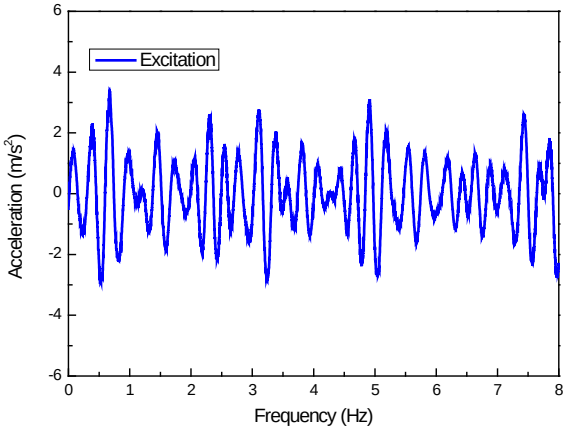

(a) time domain

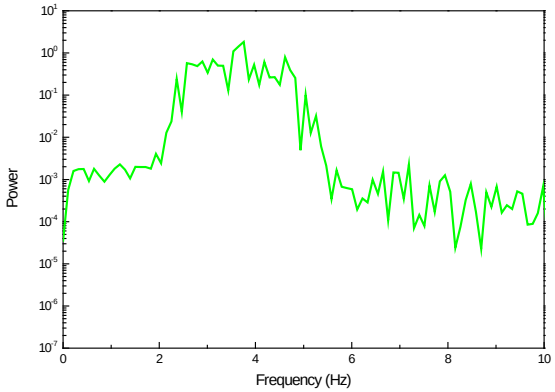

(b) frequency domain

Figure 16 Random excitation

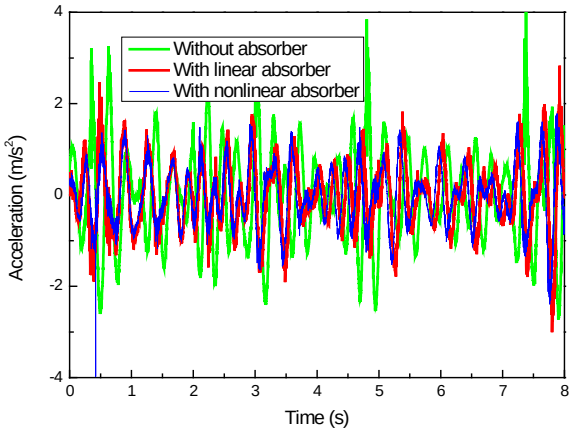

(a) time domain

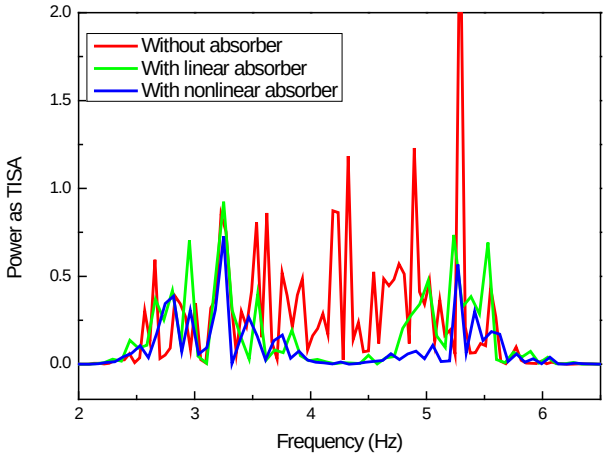

(b) frequency domain

Figure 17 Acceleration responses of the top level.

In order to evaluate the vibration absorption capability, two kinds of tests were conducted. The first one is to compare the performance of the linear absorber (without nonlinear component under 4A current) and the nonlinear absorber (with nonlinear component under 4A current) under a random excitation; the second one is to demonstrate the controllability of the hybrid MRE absorber.

Comparison between linear and nonlinear MRE absorber.

A random excitation was used to compare the performances of passive linear and passive nonlinear MRE absorbers. The random excitation signal is indicated in both time domain and frequency domain in Figure 16. From its spectrum it can be seen that its power mainly concentrates between 2Hz and 5Hz. This frequency range covers the resonance frequency range of the linear and nonlinear MRE absorber (please see Figure 11 and 12) and thus the absorption evaluation will be more persuasive. Figure 17 shows the acceleration performance of the top level of the building model in time domain and frequency domain under the random excitation. Three tests were conducted: the first one is without an absorber; the second one is with a linear absorber, and the third one is with a nonlinear absorber. It can be seen from Figure 17 (a) that the top level of the building has the smallest acceleration with nonlinear absorber. And when the

building was with the linear absorber, the acceleration is bigger than that with the nonlinear absorber but smaller than without the absorber. The spectrum of the acceleration shown in Figure 17 (b) shows the same performance that the acceleration of the top level with the nonlinear absorber has the least power distribution. The above analysis verified the nonlinear MRE absorber performs better than linear absorber under consistant current.

The Contrability evaluation of the hybrid MRE absorber

In order to evaluate the contrability of the hybtrid MRE absorber, a sweep excitation was used to excite the building. As shown in Figure 18, the excitation is designed to sweep from 5.5 Hz to 2Hz with 1m/s^2 acceleration and this frequency range covers the resonance frequency range of the hybrid MRE absorber. In order to make sure that the excitation amplitude stabilizes at 1m/s^2 from 5.5Hz to 2Hz, we started the sweep excitation from 7Hz. The performance of the proper controlled nonlinear MRE absorber on vibration attenuation for the scaled building is evaluated. The control method used here is a short time Fourier transform (STFT) control algorithm. A detailed explanation for the STFT is given by equations 12-15 (Sun et al., 2015b).

First, the time segment should be obtained by multiplying the signal x(t) by a window function h(t):

$$x_\tau(t) = x(t)h(t-\tau) \qquad (12)$$

where t is the running time, and τ is the fixed time. The window function was chosen as the hamming window, and then the Fourier transform for the modified signal is calculated as:

$$X_\tau(\omega) = \frac{1}{\sqrt{2\pi}}\int x(t)h(t-\tau)e^{-j\omega t}dt \qquad (13)$$

The energy density of the windowed signal at the fixed time τ is

$$P(\tau,\omega) = |X_\tau(\omega)|^2 = \left|\frac{1}{\sqrt{2\pi}}\int x(t)h(t-\tau)e^{-j\omega t}dt\right|^2 \qquad (14)$$

which can provide the time–frequency distribution. Then the instantaneous frequency at time τ is given by

$$\langle\omega\rangle_\tau = \frac{1}{|x(\tau)|^2}\int \omega\,|X_\tau(\omega)|^2 d\omega \qquad (15)$$

The acquired top floor acceleration was processed by the STFT algorithm in order to obtain the vibration frequency. This algorithm produces a current output by equaling the natural frequency of the absorber to the excitation frequency. Upon receiving the current signal, the absorber will adjust its stiffness to track the excitation frequency. The acceleration transmissibility from the excitation to the top plate was calculated so as to evaluate the vibration reduction effectiveness. The desired scenarios demonstrated by the transmissibility would be when the value of transmissibility reaches the lowest level. This means that the top plate's acceleration would be suppressed the most when the transmissibility reaches the minimum which is the optimal vibration absorption point of the absorber. As a comparison, three passive nonlinear absorbers which were under constant currents (0A, 2A, and 4A) were evaluated. The performance of the building without absorber is also evaluated.

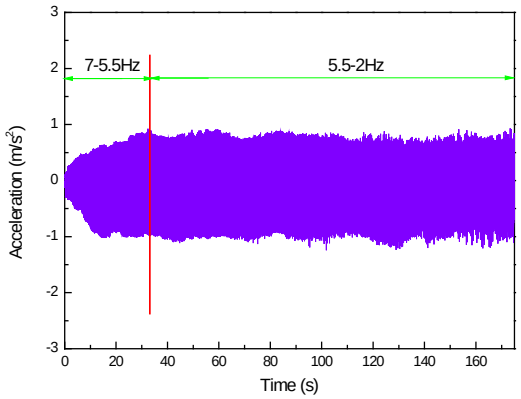

Figure 18 Sweep excitation in time domain

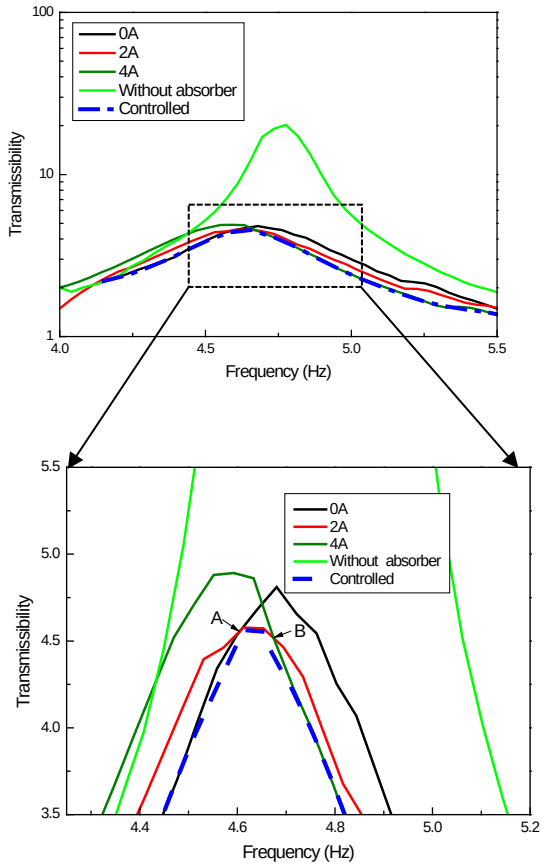

Figure 19 The comparison between passive absorbers and controlled hybrid MRE absorber

Figure 19 shows the acceleration transmissibility under all the cases. It is seen that the acceleration transmissibility of the top level of the building without the absorber has the biggest value almost over the whole frequency range. This means that the absorbers are effective on reducing the vibration energy transmissibility. For these three passive cases (0A, 2A, and 4A), before the frequency of point A, it can be seen that the absorber has the best absorption effectiveness when the current is 0A. However, when the frequency is between the point A and B, the absorber performs best under the current of 2A. Then after the point B, the absorber shows the most effective absorption when the current is 4A. Then a desired transmissibility would be one that connects these three best absorption segments. When the absorber is controlled by STFT, it can be seen from Figure 19 that the transmissibility remains at the lowest level through all the frequency range, as shown by the blue dashed line. This means that this absorber under STFT can find the optimal parameters in real time to achieve the best absorption effectiveness.

Conclusions

This study incorporated the magnetic nonlinearity into the linear MRE absorber, aiming at further broadening its operating bandwidth under each constant current. The adaptability for the linear absorber and nonlinear absorber were both verified and evaluated. Afterwards, the absorption effectiveness of this nonlinear MRE absorber on vibration control was experimentally carried out by subjecting the absorber to the random excitation and the sweep excitation. The testing results under the random excitation demonstrate that the nonlinear absorber has better absorption performance than the linear one. The results under the sweep excitation show that the nonlinear absorber controlled by STFT outperforms all the passive absorbers.

Acknowledgements

This research is supported by ARC Linkage Grants (LP160100132, No. 150100040). Dr. M. S. Cincotta is thanked for the help of language edition.

References

ARNOLD, F. 1955. Steady-state behavior of systems provided with nonlinear dynamic vibration absorbers. Journal of Applied Mechanics, 22, 487-492.

DAVIS, C. L. & LESIEUTRE, G. A. 2000. An actively tuned solid-state vibration absorber using capacitive shunting of piezoelectric stiffness. Journal of sound and vibration, 232, 601-617.

DENG, H.-X. & GONG, X.-L. 2008. Application of magnetorheological elastomer to vibration absorber. Communications in Nonlinear Science and Numerical Simulation, 13, 1938-1947.

DENG, H.-X., GONG, X.-L. & WANG, L.-H. 2006. Development of an adaptive tuned vibration absorber with magnetorheological elastomer. Smart materials and structures, 15, N111.

Yildirim, T., Ghayesh, M. H., Li, W., Alici, G. 2016. Experimental nonlinear dynamics of a geometrically imperfect magneto-rheological elastomer sandwich beam. Composite Structures, 138, 381-390.

GINDER, J. M., SCHLOTTER, W. F. & NICHOLS, M. E. Magnetorheological elastomers in tunable vibration absorbers. SPIE's 8th Annual International Symposium on Smart Structures and Materials, 2001. International Society for Optics and Photonics, 103-110.

H, F. 1911. Device for Damping Vibration of Bodies. 989958.

LEE, E., NIAN, C. & TARNG, Y. 2001. Design of a dynamic vibration absorber against vibrations in turning operations. Journal of Materials Processing Technology, 108, 278-285.

LEVITT, M. 2001. Spin Dynamics: Basics of Nuclear Magnetic Resonance. Chichester: John Wiley & Sons.

LI, Y. & LI, J. 2015. Finite element design and analysis of adaptive base isolator utilizing laminated multiple magnetorheological elastomer layers. Journal of Intelligent Material Systems and Structures, 1045389X15580654.

LI, Y., LI, J., LI, W. & DU, H. 2014. A state-of-the-art review on magnetorheological elastomer devices. Smart Materials and Structures, 23, 123001.

LIAO, G., GONG, X., KANG, C. & XUAN, S. 2011. The design of an active–adaptive tuned vibration absorber based on magnetorheological elastomer and its vibration attenuation performance. Smart materials and structures, 20, 075015.

LIU, K. & LIU, J. 2005. The damped dynamic vibration absorbers: revisited and new result. Journal of sound and vibration, 284, 1181-1189.

Mills, R.S., 1979, Model Tests on Earthquake Simulators: Development and Implementation of Experimental Procedures, Report No. 39, Blume Earthquake Engineering Center, Stanford University

PENG, C. & GONG, X. L. Active-adaptive vibration absorbers and its vibration attenuation performance. Applied Mechanics and Materials, 2013. Trans Tech Publ, 262-267.

POPP, K. M., KR GER, M., HUA LI, W., ZHANG, X. Z. & KOSASIH, P. B. 2010. MRE properties under shear and squeeze modes and applications. Journal of Intelligent Material Systems and Structures, 21, 1471-1477.

ROBERSON, R. E. 1952. Synthesis of a nonlinear dynamic vibration absorber. Journal of the Franklin Institute, 254, 205-220.

SNOWDON, J. 1959. Steady‐State Behavior of the Dynamic Absorber. The Journal of the Acoustical Society of America, 31, 1096-1103.

STAROSVETSKY, Y. & GENDELMAN, O. 2008. Dynamics of a strongly nonlinear vibration absorber coupled to a harmonically excited two-degree-of-freedom system. Journal of sound and vibration, 312, 234-256.

SUN, S., DENG, H., YANG, J., LI, W., DU, H. & ALICI, G. 2015a. Performance evaluation and comparison of magnetorheological elastomer absorbers working in shear and squeeze modes. Journal of Intelligent Material Systems and Structures, 1045389X14568819.

SUN, S., DENG, H., YANG, J., LI, W., DU, H., ALICI, G. & NAKANO, M. 2015b. An adaptive tuned vibration absorber based on multilayered MR elastomers. Smart Materials and Structures, 24, 045045.

SUN, S., YANG, J., LI, W., DENG, H., DU, H. & ALICI, G. 2015c. Development of an MRE adaptive tuned vibration absorber with self-sensing capability. Smart Materials and Structures, 24, 095012.

TANG, L. & YANG, Y. 2012. A nonlinear piezoelectric energy harvester with magnetic oscillator. Applied Physics Letters, 101, 094102.

WALSH, P. & LAMANCUSA, J. 1992. A variable stiffness vibration absorber for minimization of transient vibrations. Journal of sound and vibration, 158, 195-211.

WEBER, F. 2014. Semi-active vibration absorber based on real-time controlled MR damper. Mechanical Systems and Signal Processing, 46, 272-288.

XING, Z.-W., YU, M., FU, J., WANG, Y. & ZHAO, L.-J. 2015. A laminated magnetorheological elastomer bearing prototype for seismic mitigation of bridge superstructures. Journal of Intelligent Material Systems and Structures, 1045389X15577654.

YANG, J., DU, H., LI, W., LI, Y., LI, J., SUN, S. & DENG, H. 2013. Experimental study and modeling of a novel magnetorheological elastomer isolator. Smart Materials and Structures, 22, 117001.

YANG, J., SUN, S., DU, H., LI, W., ALICI, G. & DENG, H. 2014a. A novel magnetorheological elastomer isolator with negative changing stiffness for vibration reduction. Smart Materials and Structures, 23, 105023.

YANG, Z., QIN, C., RAO, Z., TA, N. & GONG, X. 2014b. Design and analyses of axial semi-active dynamic vibration absorbers based on magnetorheological elastomers. Journal of Intelligent Material Systems and Structures, 1045389X13519002